Third harmonic conversion efficiency from laser-dense plasma interactions

R. Ondarza
Instituto Nacional de Investigaciones Nucleares,
Apartado Postal 18-1027, México 11801, D.F., Mex.

Recibido el 10 de febrero de 2005; aceptado el 27 de junio de 2005

A perturbative nonlinear procedure is used to account for the conversion efficiency of the third harmonic reflected from a dense plasma illuminated by a short laser pulse. It is found that the power ratio of the third harmonic to that of the fundamental is given by $P_3/P_0 \sim a_0^4\,(\omega_0/\omega_p)^2$, where a_0 is the amplitude of the incident wave, and ω_0 and ω_p are the optical and plasma frequency, respectively. This power ratio was found to be in agreement with particle-in-cell (PIC) simulations. Furthermore, the model presented here predicts a resonant enhancement around a density four times critical. This effect is captured as well by numerical simulations, and proved to be a distinctive feature in the radiation spectra.

Keywords: Laser-plasma interaction; high harmonic generation.

Se emplea un método perturbativo para calcular la eficiencia en la emisión del tercer armónico por reflexión de un plasma denso en la interacción de un pulso corto de luz láser. Se encuentra que la potencia emitida está dada por $P_3/P_0 \sim a_0^4\,(\omega_0/\omega_p)^2$, donde a_0 es la amplitud de la onda incidente, ω_0 y ω_p son las frecuencias óptica y del plasma, respectivamente. La potencia obtenida se encuentra en concordancia con aquella observada por medio de la simulación numérica de partículas. Además, el método aquí presentado predice un efecto resonante alrededor de una densidad de plasma que corresponde a cuatro veces su valor crítico. Este efecto se observa, así mismo, en las simulaciones numéricas, siendo una característica distintiva en los espectros de emisión.

Descriptores: Interacción plasma-láser; generación de armónicos

PACS: 52.50.Jm; 52.65.Rr; 52.25.Os

1. Introduction

The physics of laser-dense plasma interaction involves a vast number of phenomena that may occur when a target medium is irradiated by a light source. Among the physical processes that can be found in these types of interactions we have, for instance, ionization, generation of large amplitude plasma waves, magnetic field generation, hole boring, particle acceleration, collisional absorption, and vacuum heating. Threshold intensities of these interaction phenomena have been well known throughout the development of laser technology.

The main aspect of interest to us in the interaction physics of laser pulses with overdense plasmas is harmonic generation. Radiation emission from targets irradiated by laser pulses may offer promising applications in many research fields, such as those for the development of short coherent x-ray sources [1,2].

Harmonic radiation has been under study over the past, and a considerable amount of research work is now reported in the literature. The first report on strong emission detecting up to the 46th harmonic was due to Carman and coworkers [3,4], from the irradiation of carbon targets by CO_2 laser pulses at intensities of above 5×10^{14} W/cm^2. The emission spectra from those observations showed a cutoff at a maximum harmonic number that was interpreted as corresponding to the upper shelf density of the steepened plasma profile, with emission due to nonlinear resonance absorption. Later numerical simulations provided no evidence of a cutoff for higher input intensities, with emission extending to regions in the xuv regime [5]. Moreover, laboratory experiments have detected emission at high harmonic orders, showing a rolloff of emission lines. For instance, harmonic emission at orders up to the 75th for obliquely incident Nd light pulses of duration 2.5 ps at 10^{19} W/cm^2 has been observed [6]. Further experiments have confirmed high order laser harmonics emitted with conversion efficiency decreasing in intensity with increasing order [7,8]. Another possible source of emission is known as vacuum heating [9], which corresponds to the acceleration of electrons that are pulled out of the plasma by the longitudinal component of the laser electric field. In a time of about half an optical cycle, the electric field reverses its direction and reinjects the electrons into the plasma. This strong acceleration takes place near the plasma-vacuum interface, and is thought to be responsible for part of the emission. Another mechanism for harmonic generation suggests a phase modulation of the reflected laser light from an oscillating interface [10]. Using a 'moving mirror' model, Lichters *et al.* [11] modulated the surface oscillations using Fourier components of adjustable amplitudes, and reproduced the spectra computed numerically. A complete account of harmonic emission can be found in the review paper by Gibbon [12].

More recent work has reported modulation for the harmonic emission at high intensities from solids irradiated by femtosecond laser pulses [13]. The modulation was shown to be produced by high order oscillation modes of the critical plasma frequency, and proved to be dependent on both the initial scale length and field amplitude. This radiation phenomenon could provide a means of studying the dynamics of the critical layer, and would offer a diagnostic technique in experiments.

Plasma emission from overdense plasmas has recently been observed from laser-produced plasmas by Teubner *et al.* [14], and PIC simulations by Lichters *et al.* [15] and Ondarza *et al.* [16-17]. The harmonic spectra, in these cases, are characterized by a strong emission at the plasma frequency.

In this paper, we report on the conversion efficiency for the third laser harmonic reflected from an overdense plasma irradiated by a short laser pulse at normal incidence. The power ratio is obtained from a perturbation model that uses the amplitude of a relatively weak laser field, calculated at the critical layer of a dense plasma. We have employed a similar procedure to the one followed in the model proposed by Wilks *et al.* [18], but used a different method and approximation to solve the equations that govern the density fluctuation.

The remainder of this work presents, in Sec. 2, the perturbation analysis used for the calculation of the reflected power of the third harmonic. In Sec. 3, a brief account of the simulation method is given. The discussion of the results is presented in Sec. 4, and conclusions are addressed in Sec. 5.

2. Perturbation analysis

We consider a dense plasma of a very steep density profile irradiated by an electromagnetic plane wave, linearly polarized, propagating in the z direction, with the ion density n_0 regarded as a neutralizing uniform background. The incident wave can be described by the electromagnetic vector potential **a**, whereas the electron dynamics by a cold fluid model under the assumption that the electron quiver velocity $\boldsymbol{v} = c\boldsymbol{a}/\gamma$ is greater than the electron thermal speed. Here, $\boldsymbol{a} = e\boldsymbol{A}/m_0 c^2$ is the normalized vector potential with magnitude $a \sim 8.5\,(I_{18})^{1/2}\,\lambda_L$, where I_{18} is the field intensity (measured in units of 10^{18} W/cm^2) and λ_L the wavelength in microns. The speed of light in vacuum is represented by c, m_0 and e are the electron rest mass and charge, respectively, and γ is given by $\gamma = \left[(1+a^2)/(1-v_z^2)\right]^{1/2}$, with v_z being the parallel velocity.

Using Maxwell equations and the conservation of canonical momentum, the electromagnetic wave equation can be expressed as

$$\Box^2\,\boldsymbol{a} \;=\; k_p^2\,\frac{n}{n_0}\,\frac{\boldsymbol{a}}{\gamma}\;, \tag{1}$$

where

$$\Box^2 = \frac{\partial^2}{\partial z^2} - \frac{1}{c^2}\frac{\partial^2}{\partial t^2},$$
$$k_p = \omega_p/c,$$
$$\omega_p = \left(4\,\pi\,n_0\,e^2/m_0\right)^{1/2}$$

is the plasma frequency and n the electron density.

We follow a perturbative expansion and express the vector potential to second order as $a = a_{z,0} + \epsilon\,a_{z,3} + O(\epsilon^2)$, where $a_{z,0}$ and $a_{z,3}$ represent the fundamental wave and the third laser harmonic, with amplitudes a_0 and a_3, respectively. The parameter ϵ is used to separate the terms among different orders. The density perturbation δn gives a relation $n = n_0 + \delta n$, to first order. The basic assumption is to consider both $a_0^2 \sim \epsilon$ and $\delta n \sim \epsilon$. Using this ordering, the expansion of Eq. (1) is given by

$$\left(\Box^2 - k_p^2\right) a_{z,0} = 0, \tag{2}$$

$$\left(\Box^2 - k_p^2\right) a_{z,3} = k_p^2 a_{z,0}\left(\frac{\delta n}{n_0} - \frac{1}{2}a_{z,0}^2\right), \tag{3}$$

$$\left(\Box^2 - k_p^2\right) a_{z,5} = k_p^2\left\{a_{z,3}\left(\frac{\delta n}{n_0} - \frac{3}{2}a_{z,0}^2\right) - \frac{1}{2}\frac{\delta n}{n_0}a_{z,0}^3\right\}, \tag{4}$$

where we have obtained the wave equations for the fundamental, the 3rd and 5th harmonics to orders 0, ϵ and ϵ^2, respectively. We leave for another publication the calculation for the fifth harmonic.

The electron dynamics is described by the set of equations

$$\frac{\partial n}{\partial t} + \frac{\partial}{\partial z}\left(n\,v_z\right) = 0, \tag{5}$$

$$\frac{\partial^2 \phi}{\partial z^2} = k_p^2\left(\frac{n}{n_0} - 1\right), \tag{6}$$

$$\frac{\partial p_z}{\partial t} + \frac{\partial}{\partial z}\left(m_0\,c^2\,\gamma - e\,\phi\right) = 0, \tag{7}$$

where $\phi(z)$ is the electrostatic potential.

Using the equations above, we arrive, after linearizing the continuity equation and eliminating the terms of second order, at the dynamic equation for δn

$$\frac{\partial^2 \delta n}{\partial\, t^2} + \omega_p^2\,\delta n = \frac{n_0}{2}\,c^2\,\frac{\partial^2\, a_{z,0}^2}{\partial z^2}. \tag{8}$$

To obtain the solution for the density perturbation, we first calculate the amplitude of the wave at the skin depth of the plasma. We assume that the incident, reflected, and transmitted waves can be expressed in the form

$$A_i = a_0\;\cos\left(kz - \omega_0 t\right), \tag{9}$$

$$A_r = a_r\,\cos\left(-kz - \omega_0 t + \phi_1\right), \tag{10}$$

$$A_t = a_t\,e^{-z/\delta}\,\cos\left(-\omega_0 t + \phi_2\right), \tag{11}$$

where a_0, a_r and a_t are the corresponding field amplitudes, $k = \omega_0/c$ and $\delta = \sqrt{c^2/(\omega_p^2 - \omega_0^2)}$ is the skin depth, with ω_0 the fundamental frequency. Phases ϕ_1 and ϕ_2 can be evaluated requiring that the wave and its derivatives be continuous at the surface, from which we obtain that

$$\tan\phi_1 = \frac{2\,\delta\,k}{1 - \delta^2\,k^2}, \tag{12}$$

$$\tan\phi_2 = -\frac{1}{\delta\,k}\;. \tag{13}$$

From these equations, we have that the amplitudes are related by

$$a_r{=}{-}a_0,$$

$$a_t{=}2\left(\frac{\omega_0}{\omega_p}\right) a_0,$$

which gives the transmitted wave

$$A_t = 2\left(\frac{\omega_0}{\omega_p}\right) a_0\, e^{-z/\delta}\, \cos\left(-\omega_0 t + \phi_2\right). \qquad (14)$$

Equation (14) is a solution of Eq. (2), for propagation inside the plasma.

We solve for δn, replacing $a_{z,0}$ in (8) by A_t, to account for the field amplitude that drives the density oscillations, and get

$$\delta n(t) = 4\, n_0\, \beta^2\, (1-\beta^2)\, a_0^2\, e^{-2z/\delta} \left\{1 + \frac{1}{1-4\beta^2} \times \left(2\left(2\beta^2-1\right)\cos\omega_p t + \cos 2\,\omega_0 t\right)\right\}, \qquad (15)$$

where $\beta = \omega_0/\omega_p$.

Thus the electron density oscillates at both the plasma frequency and at $2\,\omega_0$, which corresponds to the oscillation frequency of the ponderomotive force. From this solution, a resonance effect at a density four times critical can be inferred. Numerical simulations were performed to account for the reflected emission, with the result of this effect being captured as well in the spectra.

Considering only the oscillation mode at $2\,\omega_0$ in Eq. (15) we get, after substituting in Eq. (3), the source term at frequency $3\,\omega_0$ that drives the third harmonic wave,

$$\left(\Box^2 - k_p^2\right) a_{z,3} = \frac{3\,\beta^2\, k_p^2\, a_0^3}{1-4\,\beta^2}\, e^{-3z/\delta}\, \cos 3\,\omega_0 t, \qquad (16)$$

where we have not retained oscillation modes at other frequencies. This equation can be regarded as in the form of a Klein-Gordon-type equation, for a nonlinear wave $u(z,t)$ governed by

$$u_{tt} - c^2 u_{zz} + \lambda^2\, u = \epsilon\, F(u, u_t, u_z), \qquad (17)$$

where c and λ are constants and F given by the right hand side of Eq. (16).

We seek a solution in the form

$$u = a_0\, e^{-z/\delta}\, \cos\psi + \epsilon\, e^{-3z/\delta}\, a_3(a_0, \psi) + O(\epsilon^2),$$

with $\psi = \omega_0 t$, and follow a perturbative procedure to solve the wave equation for the third harmonic a_3.

Retaining all terms of order ϵ, we obtain the amplitude for the third harmonic wave as

$$a_3 = \frac{3}{8}\, \frac{\beta\, a_0^3}{1-4\,\beta^2}\, \cos 3\psi. \qquad (18)$$

The ratio of the power in the nth harmonic, P_n, to the power in the pump radiation field P_0, is given by

$$P_n/P_0 = n^2\, a_n^2/a_0^2.$$

Hence, the power ratio for the third harmonic is given by

$$\frac{P_3}{P_0} = \left(\frac{9}{8}\right)^2 \left(\frac{\omega_0\,\omega_p}{\omega_p^2 - 4\,\omega_0^2}\right)^2 a_0^4. \qquad (19)$$

3. Particle simulations

For plasma simulations we have implemented a 1 1/2-D electromagnetic particle kinetic code following the numerical algorithms developed by Birdsall and Langdon [19,20]. The integration of the equations of motion for a large number of particles is accomplished through efficiently designed numerical algorithms that solve at each time step the interaction of an external electromagnetic field and the self-consistent field quantities from the charges in the system and then use the force to move the plasma particles.

The electrostatic fields are calculated from the initial charge distribution and current densities and then recalculated from the new particle positions and velocities. A finite-difference scheme for the Lorentz equations of motion in a spatial grid, centered in time, is used to compute the electric force that accelerates the particles, and then a rotation of the particle velocities is performed to calculate the magnetic force. The code separates the transverse fields into left and right-going components which are advanced in time by adding the current densities computed from the particle velocities assigned to the grid. The Poisson's equation is integrated directly by using fast Fourier transforms of the density at the grid points, with the longitudinal field obtained from the gradient of the inverse transform of the scalar potential. Once the field quantities have been calculated at each time step, the particles are moved, for the next cycle, with new positions and velocities.

In our simulations, the plasma occupied a simulation box extending over 4-6 laser wavelengths with 2000 spatial grid cells containing 2×10^6 particles. These simulation parameters made it possible to achieve an acceptable resolution for resolving a Debye length. The density profile was chosen to have a scale length of only a fraction of a laser wavelength to simulate a very steep density gradient at the front boundary. Two vacuum gaps of half a wavelength were placed to the left and right of the plasma boundary, to allow for particle and wave propagation.

4. Results and discussion

It follows from Eq. (19) that the conversion efficiency depends on the ratio $\beta = \sqrt{n_c/n_e}$ and scales with the wave amplitude as a_0^4. In Ref. 18, the power ratio was obtained as $P_3/P_0 \sim 0.1(a_0\,\beta)^4$, which implies a higher power for β. In that paper the physical assumption for this expression to

be valid was that $a_0\,\beta \ll 1$, in contrast with the less strict condition $a_0 < 1$, required for the perturbation expansion.

In addition, from Eq. (19), we can infer the existence of a resonance effect at a density four times critical. Figures 1 and 2 show the reflected power of the third harmonic as a function of the plasma density for a wave amplitude of $a_0 = 0.5$ and 0.6, respectively. It is shown that the power ratio, represented by a solid line, is in good agreement with PIC simulations. These figures show that resonance effects characterize the spectral region for low densities, where the conversion efficiency is higher around the density four times critical, including a prominent emission at a density that corresponds to nine times critical. The source of the emission for the latter resonance is different from that which we consider at four times critical, since the third harmonic generated at the critical density propagates further inside the plasma and is reflected at a density nine times critical.

From Eq. (19), Fig. 3 shows the conversion efficiency for the third harmonic, as a function of the laser intensity for different values of the plasma density. This plot shows that the power ratio is consistent with the expected energy saturation effect that occurs for higher field amplitudes, as shown in Fig. 4 for a PIC simulation with $n_e/n_c = 10$. A more complete account of the radiation resonance effect, described in this paper, can be found in Ref. 21, where harmonic emission at multiple orders of the fundamental is reported to exhibit resonance phenomena when a dense plasma is irradiated by a short laser pulse.

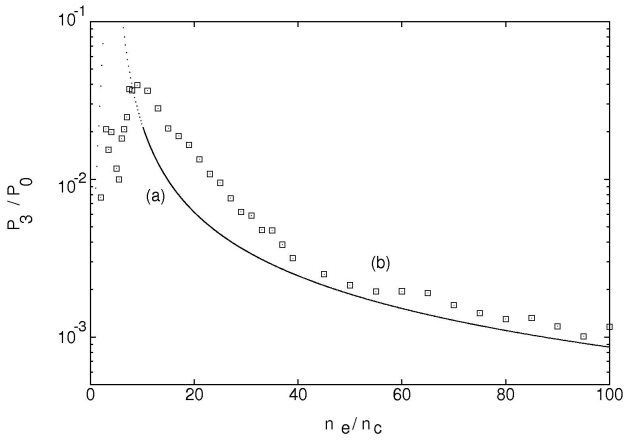

FIGURE 1. Reflected power of the 3th laser harmonic as a function of the plasma density, for $a_0 = 0.5$: (a) analytical (solid line) and (b) from simulation (squares).

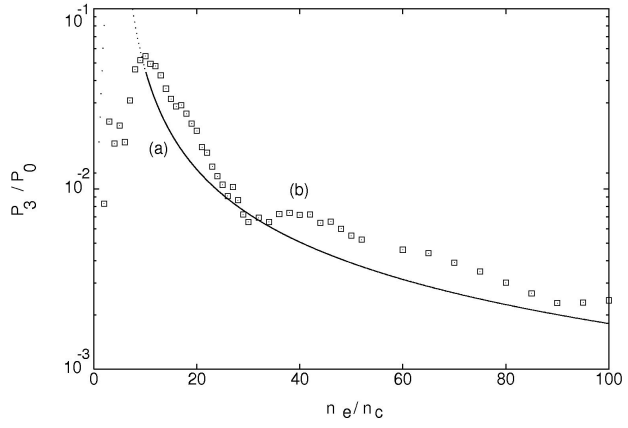

FIGURE 2. Reflected power of the 3th laser harmonic as a function of the plasma density, for $a_0 = 0.6$: (a) analytical (solid line) and (b) from simulation (squares).

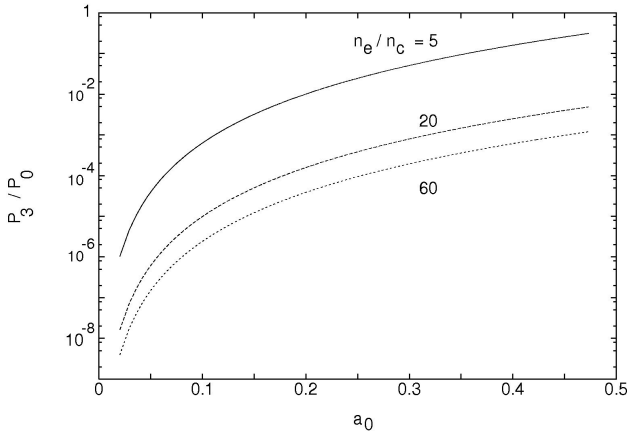

FIGURE 3. Reflected power of the 3th laser harmonic as a function of a_0, for different plasma densities.

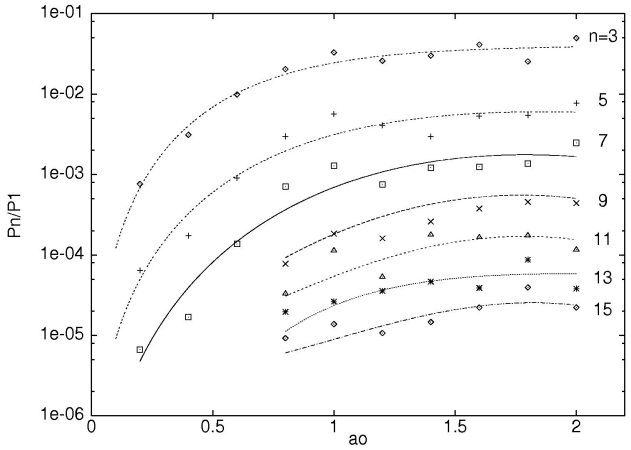

FIGURE 4. Reflected power of laser harmonics as a function of a_0, for $n_e/n_c = 10$.

5. Conclusions

A perturbative nonlinear procedure was applied to calculate the emission power for the third laser harmonic reflected from a dense plasma, illuminated at normal incidence by a laser pulse. We shall remark that the perturbation scheme employed in this analysis does not enable us to treat the case for a highly intense pulse, and is only limited by the assumption that the field strength fulfills $a_0 \leq 1$, with $a_0^2 \sim \epsilon$, for the formal perturbation expansion parameter. It was shown that the density perturbations depend on the quadratic power of the laser intensity and present oscillation modes at twice the frequency of the driver. Apart from this frequency and

intensity dependence, the density was found to resonate at 4 times critical. It was shown that this resonance effect characterizes the emission spectra, as confirmed by PIC kinetic simulations. With any perturbation expansion, confidence in the approximation diminishes as the order increases. Nevertheless, we have found in high order calculations that the pattern of resonant density emission persists, with the number of resonances increasing with the approximation order.

Furthermore, it was found that the power ratio of the third harmonic, reflected from the vacuum interface, scales with the intensity as a_0^4 and with the optical and plasma frequencies as $(\omega_0/\omega_p)^2$. The conversion efficiency found in this work can possibly be employed, as a diagnostic tool, to estimate the plasma density in experimental applications.

Acknowledgments

The author thanks Prof. T.J.M. Boyd for useful discussions and acknowledges financial support from the Consejo Nacional de Ciencia y Tecnología (CONACyT) under Contract No. 43621-F.

1. J. D. Kmetec, C. L. Gordon III, J. J. Mackin, B. E. Lemoff, G. S. Brown and S. E. Harris, *Phys. Rev. Lett.* **68** (1992) 1527.
2. F. N. Beg, A. R. Bell, A. E. Dangor, C. N. Danson, A. P. Fews, M. E. Glinsky, B. A. Hammel, P. Lee, P. A. Norreys and M. Tatarakis, *Phys. Plasmas* **4** (1997) 447.
3. R. L. Carman, C. K. Rhodes and R. F. Benjamin, *Phys. Rev.* A **24** (1981) 2649.
4. R. L. Carman, D. W. Forslund and J. M. Kindel, *Phys. Rev. Lett.* **46** (1981) 29.
5. P. Gibbon, *Phys. Rev. Lett.* **76** (1996) 50.
6. P. A. Norreys, M. Zepf, S. Moustaizis, A. P. Fews, J. Zhang, P. Lee, M. Bakarezos, C. N. Danson, A. Dyson, P. Gibbon, P. Loukakos, D. Neely, F. N. Walsh, J. S. Wark and A. E. Dangor, *Phys. Rev. Lett.* **76** (1996) 1832.
7. D. von der Linde, T. Engers, G. Jenke, P. Agostini, G. Grillon, E. Nibbering, A. Mysyrowicz and A. Antonetti, *Phys. Rev.* A **52** (1995) R25.
8. S. Kohlweyer, G. D. Tsakiris, C. -G. Wahlström, C. Tillman and I. Mercer, *Opt. Commun.* **117** (1995) 431.
9. F. Brunel, *Phys. Rev. Lett.* **59** (1987) 52.
10. S. V. Bulanov and N. M. Naumova, *Phys. Plasmas* **1** (1994) 745.
11. R. Lichters, J. Meyer-ter-Vehn and A. Pukhov, *Phys. Plasmas* **3** (1996) 3425.
12. P. Gibbon, *IEEE J. Quantum Electron.* **33** (1997) 1915.
13. I. Watts, M. Zepf, E. L. Clark, M. Tatarakis, K. Krushelnick, A. E. Dangor, R. M. Allot, R. J. Clarke, D. Neely and P. A. Norreys, *Phys. Rev. Lett.* **88** (2002) 155001.
14. U. Teubner, D. Altenbernd, P. Gibbon, E. Förster, A. Mysyrowicz, P. Audebert, J. -P. Geindre, J. -C. Gauthier, R. Lichters and J. Meyer-ter-Vehn, *Opt. Commun.* **144** (1997) 217.
15. R. Lichters and J. Meyer-ter-Vehn, *Multiphoton Processes* (Institute of Physics Publishing, Bristol and Philadelphia, 1997).
16. R. Ondarza-Rovira and T. J. M. Boyd, *Phys. Plasmas* **7** (2000) 1520.
17. T. J. M. Boyd and R. Ondarza-Rovira, *Phys. Rev. Lett.* **85** (2000) 1440.
18. S. C. Wilks, W. L. Kruer and W. B. Mori, *IEEE Trans. Plasma Sci.* **21** (1993) 120.
19. C. K. Birdsall and A. B. Langdon, *Plasma Physics via Computer Simulation*, (Institute of Physics Publishing, Bristol and Philadelphia, 1995).
20. A. B. Langdon and B. F. Lasinski, *Meth. Comput. Phys.* **16** (1976) 327.
21. R. Ondarza, *Phys. Rev.* E **67** (2003) 066401.